J Exp Neurol. 2026;7(2):93–100.

Journal of Experimental Neurology Commentary

Resolving Glycosphingosine Isomers by Crown Ether–Assisted Ion Mobility for Neurological Lipidomics

Chao Pang[1], Sanaz Mohammadzadeh Koumleh[1], David V. Dearden[1], Kenneth W. Lee[1,*]

[1]Brigham Young University, Provo, UT, 84602, USA

[*]Correspondence should be addressed to Kenneth W. Lee, Kenny.Lee@byu.edu

Received date: May 08, 2026, **Accepted date:** June 22, 2026

Citation: Pang C, Koumleh SM, Dearden DV, Lee KW. Resolving Glycosphingosine Isomers by Crown Ether–Assisted Ion Mobility for Neurological Lipidomics. J Exp Neurol. 2026;7(2):93–100.

Abstract

Glycosphingosines are neuroactive lipids whose stereochemical variations are increasingly implicated in neuronal dysfunction and neurodegenerative disease processes. However, their close structural similarity renders stereoisomer-resolved analysis inaccessible to conventional LC–MS approaches, limiting mechanistic interpretation of lipid-associated neuropathology. In previous work, we demonstrated that complexation of glycosphingosine isomers with crown ethers enabled cyclic ion mobility spectrometry to resolve most of the species. Here, we investigate the energetics and structural effects of crown ether binding to interrogate the mechanism of separation enhancement. Systematic evaluation of crown ether derivatives shows that separation efficiency does not scale with macrocycle size or structural complexity, but is maximized by 18-crown-6, indicating a geometry-dependent interaction. Molecular modeling supports a mechanism in which the protonated amine preferentially associates with the crown ether cavity and further induces conformational reorganization rather than simple collision cross-section expansion. Saccharide-driven reactivity in boronic acid–diols interaction provided complementary modification of glycosphingosine sugar headgroups to further enhance isomer discrimination. The combination of noncovalent sphingosine backbone modification via crown ether complexation and covalent sugar headgroup modification provides a tunable analytical platform for stereochemistry-resolved glycosphingolipid analysis and may facilitate more precise characterization of lipid species implicated in neurodegenerative disease, such as alpha-synuclein aggregation and lysosomal dysfunction.

Keywords: Glycosphingolipid, Glycosphingosine, Stereoisomer, Crown ether, Ion mobility, Mass spectrometry

Commentary

Glycosphingosines (GlycoSphs) occupy a distinctive position at the intersection of lipid metabolism [1], membrane biophysics [2], and neurobiology [3], and thereby uniquely influence both cellular homeostasis [4] and neurodegenerative vulnerability [5]. Among these, glucosylsphingosine (GlcSph) and galactosylsphingosine (GalSph) have emerged as particularly important neuroactive lipids whose stereochemical variations are increasingly recognized as critical determinants in disease-relevant mechanisms [6]. Accumulating evidence suggests that these pathological effects are not dictated solely by total lipid abundance but are critically modulated by subtle stereochemical features of both the sphingoid backbone [7] and sugar headgroup [8].

This structure–function relationship is evident across lysosomal [9] and neurodegenerative disorders [10]. In neuronopathic Gaucher disease, elevated GlcSph levels are directly linked to neuronal toxicity, lysosomal stress [11], impaired autophagy [12], and early-onset neurodegeneration [13]. Beyond classical lysosomal storage disorders, GlcSph is mechanistically relevant in broader neurodegenerative contexts [14], most notably in GBA1-associated Parkinson's disease, where it promotes α-synuclein aggregation [15–18], disrupts neuronal homeostasis [19], correlating with disease severity [20] and motor complications [21].

GalSph is well established as a potent neurotoxin in Krabbe disease, driving oligodendrocyte death [22,23], demyelination [24], axonal transport disruption [25], and neuroinflammatory activation of microglia [26] and astrocytes [27]. Collectively, these observations demonstrate that GlycoSphs function not merely as metabolic byproducts, but as bioactive lipids whose structure-dependent interactions shape neuronal vulnerability and disease progression across multiple neurological disorders

[28,29]. Therefore, accurate stereochemistry-resolved analysis of GlycoSphs is not merely an analytical challenge, but a necessity for identifying and characterizing disease states.

Despite their well-established biological importance, the close structural similarity of GlycoSph stereoisomers has rendered them largely inseparable by conventional liquid chromatography–mass spectrometry (LC–MS) [30], thereby limiting stereochemistry-aware interpretation of lipid-driven neuropathology and biomarker data [31]. Although conventional LC–MS/MS workflows are effective for bulk quantification, they generally fail to resolve GlycoSph stereoisomers that differ in anomeric configuration or subtle hydroxyl orientation [32,33].

Consequently, isomer-specific biological effects are either inferred or ignored when analyzing clinically relevant matrices including plasma [34,35], cerebrospinal fluid [31,36], and dried blood spots [37]. This analytical blind spot is consequential in neurological research, where single sugar-headgroup or sphingoid-base differences can directly perturb oligodendrocyte membrane architecture [38], alter protein recognition [39], and bias signaling pathways linked to pathological α-synuclein assembly [40]. The nearly-identical GalSph / GlcSph differs only in sugar-headgroup stereochemistry yet may exhibit distinct membrane partitioning behavior and pathological protein interactions [41]. This limitation represents a critical barrier to mechanistic interpretation in neurological lipidomics.

Recent advances in ion mobility spectrometry (IMS) have facilitated the separation of lipid stereoisomers based on gas-phase conformational differences [42,43]; however, the intrinsic structural similarity of GlycoSph stereoisomers frequently precludes separation even on advanced ion mobility platforms, such as Cyclic IMS (cIMS), which provides a theoretically unlimited separation pathlength for high-resolution IMS separations [44]. The inability to achieve complete separation via high-resolution IMS indicates a need for additional strategies that amplify conformational differences among isomers [45,46]. In this context, our recent work separating GlcSph and GalSph anomers establishes an analytical framework for resolving previously hidden neuroactive stereochemical states that may shape membrane dysfunction and protein aggregation [47].

We recently demonstrated that noncovalent complexation with crown ethers enables cIMS to resolve the four GlycoSph stereoisomers glucosyl(α) sphingosine, glucosyl(β) sphingosine, galactosyl(α) sphingosine, and galactosyl(β) sphingosine [47]. These stereoisomers are structurally identical except for the orientation of the sphingosine–sugar ether linkage at the anomeric C1 position—with α referring to an axial orientation and β referring to an equatorial orientation—and the orientation of the C4 hydroxyl of the sugar headgroup, which is axial in galactosyl species and equatorial in glucosyl species. The structural similarity was apparent when attempts to resolve any binary combinations by extended path lengths in the cIMS yielded no observed separation. Interestingly, complexation with 12-crown-4 (12C4) provided no improvement in separation. Larger crown ethers, including 15-crown-5 (15C5) and 18-crown-6 (18C6), provided varying degrees of cIMS separation enhancement, indicating that crown ether size was important to the mechanism of resolution enhancement.

To further interrogate the mechanism of crown ether–assisted GlycoSph separation, a series of structurally diverse crown ether derivatives was systematically evaluated as gas-phase shift reagents. These derivatives were selected to systematically investigate how crown ether structural features influence host–guest interactions with GlycoSph and, consequently, ion mobility separation performance. The derivative panel was designed to probe several key parameters, including macrocycle cavity size, conformational flexibility, aromaticity, and the presence of additional functional groups capable of altering binding geometry. Smaller macrocycles such as 12-crown-4 and 15-crown-5 were included to evaluate the effect of reduced cavity size and coordination capability relative to 18-crown-6. Larger crown ethers, including dibenzo-21-crown-7 (DB21C7), dicyclohexyl-24-crown-8 (DCH24C8), and dibenzo-30-crown-10 (DB30C10), were selected to determine whether increasing cavity size and conformational flexibility could further enhance complex stability and stereoisomer discrimination. Aromatic derivatives such as dibenzo-21-crown-7 were also expected to introduce additional rigidity and potential π-interactions that might influence guest orientation. Functionalized analogues, including 4′-aminobenzo-15-crown-5 and N-phenylaza-15-crown-5, were chosen to assess the impact of heteroatom substitution and additional hydrogen-bonding or electrostatic interaction sites on crown ether–GlycoSph complexation. BME-44 was included to explore the potential for interactions with two crown ether groups in promoting more complex binding and stereochemistry-dependent discrimination. Collectively, this derivative set was designed to empirically determine crown ether structural features that enhanced GlycoSph isomer separation, as well as features that appeared to have minimal effects.

Across all tested systems, separation performance was evaluated using two metrics: (i) the number of successfully resolved binary isomer pairs and (ii) the number of distinguishable peaks in four-component GlycoSph mixtures (**Figure 1**). Quantitative measures of binary mixture separations along with the ion mobility parameters that produced each result are reported in our previously published work, upon which the present commentary is based [47].

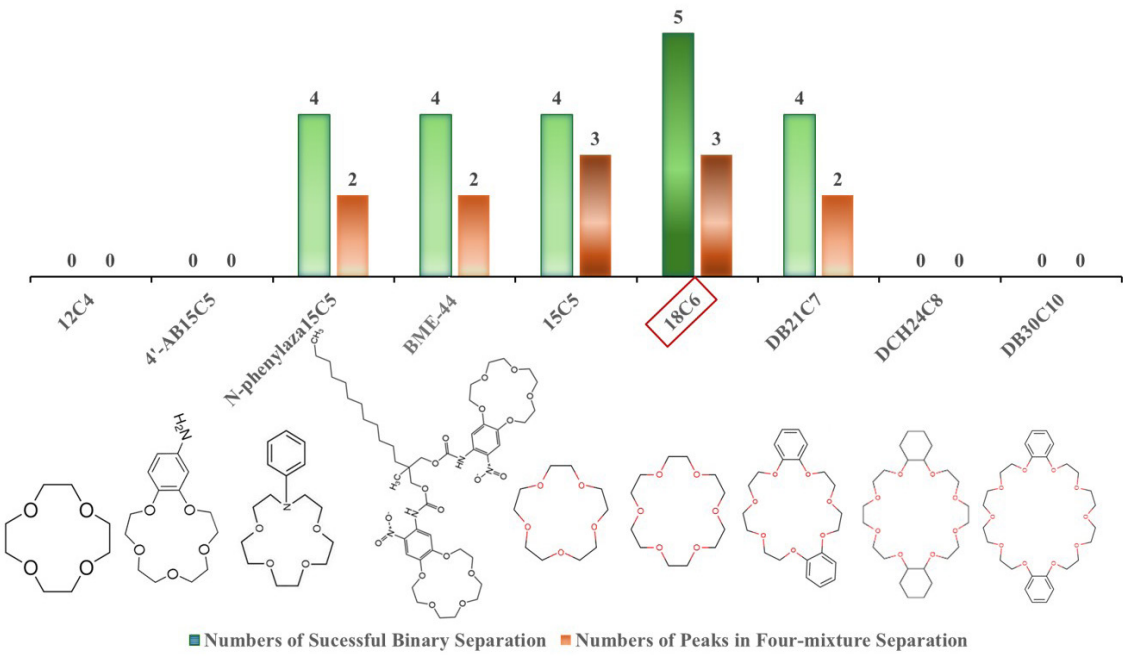

Figure 1. Representative sample of crown ether derivatives used for GlycoSph isomer separation by cIMS. The comparison of crown ether effectiveness was based on the number of successful binary separations (green bars) and the number of resolved peaks in a four-mixture separation (orange bars).

This evaluation demonstrated that small macrocycles such as 12C4 and functionalized derivatives with constrained geometries exhibited no measurable separation capability, potentially due to minimal interactions with the GlycoSph isomers. Intermediate-sized systems, particularly 15C5 and its derivatives, resolved multiple binary isomer pairs but failed to achieve complete discrimination in more complex mixtures. 18C6 resolved the greatest number of binary pairs and provided the best four-component separation, with three observable peaks. Notably, further increases in macrocycle size beyond 18C6 do not improve separation, and in some cases reduce performance, despite providing larger coordination environments. Ultimately, we identified 18C6 as the best candidate for future work; however, a better understanding of the mechanisms of binding and isomer separation enhancement is needed to either optimize current separations with 18C6 or investigate derivatives of 18C6 that could fully separate all four isomers in a single complex mixture.

Our initial attempts to elucidate any mechanistic insights relied heavily on the changing degrees of separation for isomer pairs when bound to different crown ethers. The most likely GlycoSph protonation site is the amine functional group, and, based on previous literature, a crown ether would bind the protonated amine via hydrogen bonding [48]. If this were the only intermolecular interaction, the relative changes to GlycoSph isomer cross sections would be a result of simply adding additional volume near the amine. This hypothesis would predict increased cross-sectional differences among the isomers while conserving their inherent relative structural differences. In terms of ion mobility measurements, the arrival order of GlycoSph isomers would be conserved while increasing the resolution between neighboring peaks.

Interestingly, however, the arrival order of separated isomers was not consistent for each crown ether, and the change in calculated resolution values were not monotonic as a function of crown ether identity. For example, 15C5 achieved baseline resolution equaling or exceeding 1.5 (based on the standard chromatography definition of resolution: $1.178 \times \frac{(t_2 - t_1)}{(W_1 + W_2)}$) following 31 to 41 m separation in the cIMS for binary mixtures with glucosyl(β) sphingosine, whereas binary mixtures containing any of the other three isomers resulted in weak or no separation. By contrast, DB21C7 readily achieved baseline resolution exceeding 1.5 following 31 to 41 m separation for all mixtures containing an α anomer with a β anomer; however, the two binary mixtures containing species with the same anomeric linkage (α or β) and different sugar headgroups (Glc or Gal) showed no separation. These two examples demonstrate that separation efficiency does not scale directly with crown ether size, ring flexibility, or substituent complexity [49,50]. Instead,

15C5 appears to have a unique complexation with glucosyl(β) sphingosine that differentiates it from the other isomers, and DB21C7 appears to complex differently with GlycoSph isomers primarily based on the anomeric linkage. Therefore, multiple interactions in GlycoSph–crown ether complexes appear to dictate unique geometries that produce varying results in terms of IMS separation.

Crown ethers can act as gas-phase mobility shift reagents, where selective host–guest interactions with protonated amines can reorganize ion conformations rather than merely increasing collision cross section (CCS) [49,51]. Complexation with a crown ether could have at least the following three effects: (1) The crown ether would increase the CCS because of additional bulk added to the overall structure. (2) If the crown ether complexes with the protonated amine, initial intramolecular interactions involving the protonated amine would be disrupted, resulting in conformational changes. (3) The crown ether might interact with other GlycoSph moieties in addition to the protonated amine, further resulting in conformational changes. The clear differences in separation behavior among crown ethers suggest that each crown ether produces different conformational changes via effects 2 and 3 explained above [47]. This proposed explanation, however, is merely speculative and experimental mobility data cannot provide clear structural evidence for existing interactions. In addition, the underlying assumption of initial crown ether binding position on the protonated amine, though well-founded in the literature, has not been explicitly demonstrated for GlycoSph species. To better determine the structure of GlycoSph–crown ether complexes and thereby support the mechanism of separation enhancement, we investigated the energetics of crown ether binding and additional intermolecular interactions using molecular modeling. Following structural investigation and optimization, theoretical CCS were calculated and compared to previous experiments.

To investigate structural changes due to crown ether binding, conformational searches were performed for each lipid both in the presence and absence of 18C6. The MMFF force field and a Monte Carlo search algorithm were used in Spartan to perform initial conformational searches. A maximum of 10,000 conformations were examined in the process of the conformational search and conformers within 40 kJ mol^{-1} of the lowest-energy conformer were retained, with up to 500 conformers selected for further optimization at the PM6 semi-empirical level using the default convergence criteria provided in Spartan. For GlycoSph–crown ether complexes, the lowest-energy conformer was identified to calculate the binding energies. Binding energies were then calculated based on optimized structures. Theoretical CCS values of the ten lowest energy conformers were calculated using the IMoS software package with the trajectory method and nitrogen as the buffer gas. Experimental CCS values were determined by constructing calibration curves of reported Agilent Tune Mix ion drift tube CCS vs. measured cIMS times [52].

As expected, the calculated binding energies show that 18C6 preferentially binds to the GlycoSph protonated amine. The higher stabilization can be attributed to the greater basicity of the nitrogen atom and its better ability to act as a hydrogen-bond donor, resulting in a more favorable host–guest interaction within the crown ether cavity. In the absence of 18C6, galactosyl(β) sphingosine adopts a moderately collapsed conformation, with an average theoretical CCS of 216 $Å^2$ (**Figure 2a**), which agrees well with the experimentally determined CCS of 217.4 ± 0.4 $Å^2$. Upon complexation with 18C6, the average theoretical CCS value increases to 267 $Å^2$ (**Figure 2b**), again in good agreement with the experimental value of 266.5 ± 0.4 $Å^2$. In terms of the three potential effects of crown ether complexation noted previously, an increase in CCS (effect 1) was expected. Without the presence of 18C6, the protonated amine appears to interact with sugar oxygen atoms via hydrogen-bonding; however, per effect 2, the crown ether disrupts these intramolecular interactions, causing a large conformational change. Additionally, there appear to be favorable Van der Waals interactions between the crown ether and sugar, suggested by the stacked configuration of both rings, which supports the presence of effect 3. The sphingosine tail also dramatically changes its orientation potentially due to sterics introduced by the crown ether.

Based on these initial modeling results, both the sugar headgroup and sphingosine tail differentially interact depending on the absence or presence of 18C6, leading to different spatial arrangements of the sugar headgroup and sphingosine tail. These conformational changes are likely dependent on stereochemistry; however, continued molecular modeling of GlycoSph-crown ether complexes will be investigated to validate the hypothesis that an amine-bound crown ether facilitates stereochemistry-dependent secondary reorganization of the sugar headgroup and sphingosine backbone.

This induced conformational divergence provides a more mechanistically satisfying explanation than simple CCS scaling [53] and, to our knowledge, offers the first explicit structural rationale for crown ether–assisted GlycoSph stereoisomer separation. Our experimental results within the context of our initial modeling results suggest that 18C6 provides the most favorable coordination environment for generating conformational differences among GlycoSph isomers. A major potential reason for 18C6 providing the best separation enhancement is that its symmetry results in 18C6 completely dominating the hydrogen bonding capability of the ammonium group, preventing it from interacting with the sugar headgroup or sphingosine tail. With less-appropriate symmetry, the smaller or larger crown ethers leave more

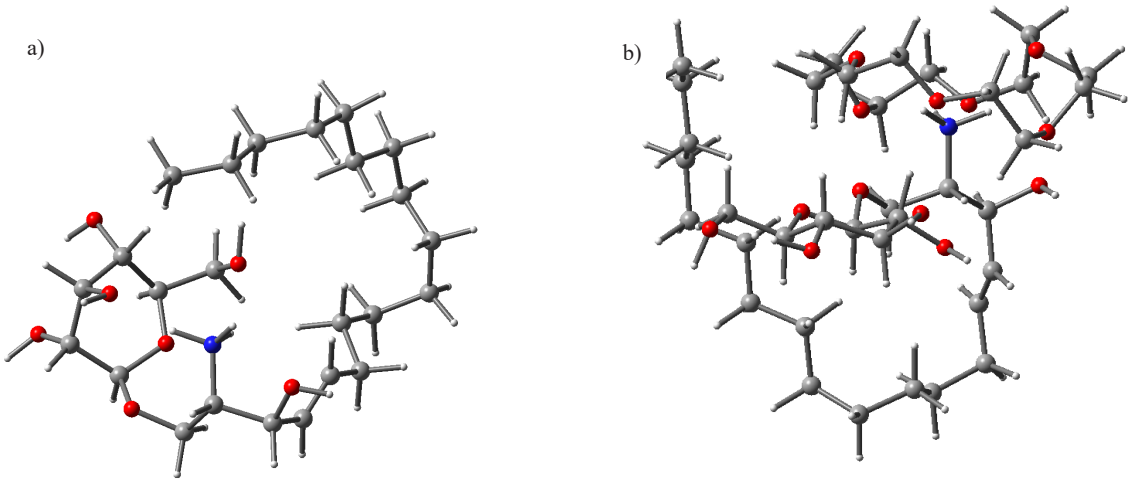

Figure 2. Representative calculated gas-phase conformations of (**a**) galactosyl(β)-sphingosine and (**b**) the corresponding galactosyl**(**β)-sphingosine/18-crown-6 complex obtained from molecular modeling. The uncomplexed glycosphingosine adopts a relatively compact conformation with a theoretical collision cross section (CCS) of 216 Å^2, whereas complexation with 18-crown-6 results in a more extended structure with a calculated CCS of 267 Å^2. The modeled interaction places the protonated amine in close association with the crown ether cavity, which is accompanied by redistribution of intramolecular interactions and altered molecular geometry. These observations are consistent with a differential stabilization mechanism in which crown ether binding favors distinct conformational populations that contribute to CCS changes and enhanced ion mobility separation. Red and blue spheres represent oxygen and nitrogen atoms, respectively.

potential for intramolecular hydrogen bonding. In addition, smaller crown ethers are less likely to support additional intermolecular interactions with other GlycoSph functional groups, while larger macrocycles potentially introduce excessive flexibility, reducing the energetic discrimination between competing conformations.

We plan to investigate additional crown ether sizes via molecular modeling. Functionalized derivatives, although structurally more complex, do not improve separation, suggesting that additional substituents do not compensate for suboptimal ring geometry. The main effect of optimal crown ether size in disrupting intramolecular hydrogen bonding via complexation with the protonated amine appears to be critical for stereochemical discrimination. This mechanistic insight provides a foundation for the rational design of future shift reagents and supports the broader concept that targeted molecular interactions can be engineered to resolve subtle stereochemical differences in biologically relevant isomers.

Whereas crown ether complexation provides a noncovalent strategy for enhancing GlycoSph isomer discrimination through ligand-induced conformational reorganization, covalent modification of the sugar headgroup offers an additional and potentially orthogonal route for amplifying structural differences. Because GlycoSph isomers differ not only in anomeric configuration but also in saccharide stereochemistry and hydroxyl orientation, selective chemical derivatization at sugar hydroxyl sites can provide an orthogonal axis for tuning separations beyond amine-directed interactions. Boronic acids exhibit reversible covalent interactions with cis-diol motifs in carbohydrates [54]. Previous reports suggest that iodophenylboronic acid (IPBA) derivatization may proceed selectively with GalSph, implying stereochemically constrained accessibility within the sugar headgroup [55]. However, the structural basis of this selectivity and the true extent of reactivity across GlcSph and GalSph remain incompletely understood.

Under optimized reaction conditions, boronic acid–diol functionalization was observed for all four species, indicating that IPBA-mediated derivatization is not inherently selective against GlcSph as previously presumed [56]. Using cIMS, we further examined IPBA-functionalized GlcSph and GalSph in both α- and β- anomeric forms. These separations were only achieved with extended separation path lengths using cIMS, emphasizing the subtle structural heterogeneity among derivatized stereoisomers. Beyond simply serving as a derivatization step for signal enhancement, boronic acid–diol functionalization potentially acts as a mechanistically informative probe of stereochemistry-dependent chemical accessibility. Detailed characterization of reaction selectivity, reaction efficiency, quantitative separation metrics, and competitive interactions will be reported separately.

Unlike crown ether complexation, which primarily exploits interactions between protonated amine groups and macrocyclic oxygen donors, IPBA derivatization directly interrogates the sugar headgroup through covalent boronate ester formation. Together, these approaches provide complementary views of GlycoSph structure: one through noncovalent conformational stabilization and the other through covalent saccharide-selective reactivity. From these results, we propose that cooperative tuning of both host–guest complexation and sugar headgroup chemistry can further amplify stereoisomer discrimination. Targeted derivatization of hydroxyl groups through boronic acid–diol functionalization offers a promising complementary strategy when paired with crown ether complexation. Rather than treating crown ether complexation as a standalone separation solution, this framework positions it as the first layer of a programmable stereochemistry-resolved lipid analysis platform, in which multiple noncovalent and covalent modifications can be rationally combined to interrogate hidden neuroactive microstates [57,58].

In conclusion, IMS separation of GlycoSph isomers is primarily enabled by strategic analyte modifications. These strategies include crown ether-induced structural reorganization arising from secondary interactions between the protonated amine-bound crown ether, the saccharide headgroup, and the sphingosine tail. Although yet to be validated, these conformational changes appear to be dependent on each isomer's stereochemistry and thereby enable cIMS separations of GlycoSph stereoisomers. Our experiments and initial modeling results suggest that crown ether separation enhancement results from an optimal crown ether geometry, rather than simply scaling with crown ether size or complexity.

Looking forward, the combination of crown ether optimization and sugar-head modification defines a flexible framework for stereochemistry-resolved lipid analysis. While crown ether–mediated separation establishes the mechanistic foundation, emerging chemical modification strategies offer complementary routes for further enhancing resolution. Beyond analytical performance, stereochemistry-resolved glycosphingolipid (GSL) analysis may facilitate future investigations into the roles of specific GSL isomers in neurodegenerative disease mechanisms, lysosomal dysfunction, neuroinflammatory signaling, and α-synuclein-associated pathology. Improved discrimination of structurally similar GSL species may also support the identification of disease-associated lipid signatures and contribute to the development of more specific lipid-based biomarkers. Continued development will enable rational design of next-generation shift reagents and chemically tuned lipid probes, providing new opportunities to interrogate structure–function relationships in glycosphingolipid biology and to advance disease-oriented studies in neurodegenerative disorders, neuronal dysfunction, neuroinflammation, and disease progression.

Funding Statement

We acknowledge support from the National Science Foundation (CHE-2403998).

Declarations

AI disclosure statement This work was supported by AI technologies, including DeepL Translate facilitated translation tasks; ChatGPT and Grammarly, which refined the language, improved clarity, and transformed the content into standardized academic English; while Perplexity, SciSpace, LitMap, and Connected Papers helped with literature searches, displaying scientific connections and contextualizing research topics. AI technology also played a role in synthesizing technical content, ensuring thematic coherence between sections, preserving the authors' scientific intent, and reducing redundancy through adaptive rephrasing and structural refinement.

Conflict of Interest

The authors declare no competing interests.

References

1. Ryckman AE, Brockhausen I, Walia JS. Metabolism of Glycosphingolipids and Their Role in the Pathophysiology of Lysosomal Storage Disorders. Int J Mol Sci. 2020 Sep 19;21(18):6881.

2. Maggio B, Fanani ML, Rosetti CM, Wilke N. Biophysics of sphingolipids II. Glycosphingolipids: an assortment of multiple structural information transducers at the membrane surface. Biochim Biophys Acta. 2006 Dec;1758(12):1922–44.

3. Belarbi K, Cuvelier E, Bonte MA, Desplanque M, Gressier B, Devos D, et al. Glycosphingolipids and neuroinflammation in Parkinson's disease. Mol Neurodegener. 2020 Oct 17;15(1):59.

4. Olson DK, Fröhlich F, Farese RV Jr, Walther TC. Taming the sphinx: Mechanisms of cellular sphingolipid homeostasis. Biochim Biophys Acta. 2016 Aug;1861(8 Pt B):784–92.

5. Mandik F, Vos M. Neurodegenerative Disorders: Spotlight on Sphingolipids. Int J Mol Sci. 2021 Nov 5;22(21):11998.

6. Hülsmeier AJ. Glycosphingolipids in neurodegeneration - Molecular mechanisms, cellular roles, and therapeutic perspectives. Neurobiol Dis. 2025 Apr;207:106851.

7. D'Auria L, Reiter C, Ward E, Moyano AL, Marshall MS, Nguyen D, et al. Psychosine enhances the shedding of membrane microvesicles: Implications in demyelination in Krabbe's disease. PLoS One. 2017 May 22;12(5):e0178103.

8. Schueler UH, Kolter T, Kaneski CR, Blusztajn JK, Herkenham M, Sandhoff K, et al. Toxicity of glucosylsphingosine (glucopsychosine) to cultured neuronal cells: a model system for assessing neuronal damage in Gaucher disease type 2 and 3. Neurobiol Dis. 2003 Dec;14(3):595–601.

9. Wald H, Cicalese S, Yao L, Hatcher N, Luo W, Shen X, et al. Glucosylsphingosine is a potential fluid-based biomarker of lysosomal dysfunction in Cln3$^{\Delta ex7/8}$ mice. Neurobiol Dis. 2025 Oct 1;214:107026.

10. Udayar V, Chen Y, Sidransky E, Jagasia R. Lysosomal dysfunction in neurodegeneration: emerging concepts and methods. Trends Neurosci. 2022 Mar;45(3):184–99.

11. van Eijk M, Ferraz MJ, Boot RG, Aerts JMFG. Lyso-glycosphingolipids: presence and consequences. Essays Biochem. 2020 Sep 23;64(3):565–78.

12. Sun Y, Grabowski GA. Impaired autophagosomes and lysosomes in neuronopathic Gaucher disease. Autophagy. 2010 Jul;6(5):648–9.

13. Srikanth MP, Jones JW, Kane M, Awad O, Park TS, Zambidis ET, et al. Elevated glucosylsphingosine in Gaucher disease induced pluripotent stem cell neurons deregulates lysosomal compartment through mammalian target of rapamycin complex 1. Stem Cells Transl Med. 2021 Jul;10(7):1081–94.

14. Bougea A. Underlying Mechanisms of GBA1 in Parkinson's Disease and Dementia with Lewy Bodies: Narrative Review. Genes (Basel). 2025 Dec 15;16(12):1496.

15. Surface M, Balwani M, Waters C, Haimovich A, Gan-Or Z, Marder KS, et al. Plasma Glucosylsphingosine in GBA1 Mutation Carriers with and without Parkinson's Disease. Mov Disord. 2022 Feb;37(2):416–21.

16. Mahoney-Crane CL, Viswanathan M, Russell D, Curtiss RAC, Freire J, Bobba SS, et al. Neuronopathic GBA1L444P Mutation Accelerates Glucosylsphingosine Levels and Formation of Hippocampal Alpha-Synuclein Inclusions. J Neurosci. 2023 Jan 18;43(3):501–21.

17. Marano M, Zizzo C, Malaguti MC, Bacchin R, Cavallieri F, De Micco R, et al. Increased glucosylsphingosine levels and Gaucher disease in GBA1-associated Parkinson's disease. Parkinsonism Relat Disord. 2024 Jul;124:107023.

18. Taguchi YV, Liu J, Ruan J, Pacheco J, Zhang X, Abbasi J, et al. Glucosylsphingosine Promotes α-Synuclein Pathology in Mutant GBA-Associated Parkinson's Disease. J Neurosci. 2017 Oct 4;37(40):9617–31.

19. Chinnappa K, Ballorin F, Francis F. Fundamental Neurochemistry Review: Sphingolipids and Ceramides in Brain Development. J Neurochem. 2025 Oct;169(10):e70262.

20. Schwartz RS, Halliday GM, Soh D, Cordato DJ, Kril JJ. Impact of small vessel disease on severity of motor and cognitive impairment in Parkinson's disease. J Clin Neurosci. 2018 Dec;58:70–4.

21. Kelly MJ, Lawton MA, Baig F, Ruffmann C, Barber TR, Lo C, et al. Predictors of motor complications in early Parkinson's disease: A prospective cohort study. Mov Disord. 2019 Aug;34(8):1174–83.

22. Cho KH, Kim MW, Kim SU. Tissue culture model of Krabbe's disease: psychosine cytotoxicity in rat oligodendrocyte culture. Dev Neurosci. 1997;19(4):321–7.

23. Haq E, Giri S, Singh I, Singh AK. Molecular mechanism of psychosine-induced cell death in human oligodendrocyte cell line. J Neurochem. 2003 Sep;86(6):1428–40.

24. O'Sullivan C, Dev KK. Galactosylsphingosine (psychosine)-induced demyelination is attenuated by sphingosine 1-phosphate signalling. J Cell Sci. 2015 Nov 1;128(21):3878–87.

25. Cantuti Castelvetri L, Givogri MI, Hebert A, Smith B, Song Y, Kaminska A, et al. The sphingolipid psychosine inhibits fast axonal transport in Krabbe disease by activation of GSK3β and deregulation of molecular motors. J Neurosci. 2013 Jun 12;33(24):10048–56.

26. Jeong YH, Kim Y, Song H, Chung YS, Park SB, Kim HS. Anti-inflammatory effects of α-galactosylceramide analogs in activated microglia: involvement of the p38 MAPK signaling pathway. PLoS One. 2014 Feb 11;9(2):e87030.

27. Brambilla R. The contribution of astrocytes to the neuroinflammatory response in multiple sclerosis and experimental autoimmune encephalomyelitis. Acta Neuropathol. 2019 May;137(5):757–83.

28. Marano M, Zizzo C, Cavallieri F, Avenali M, Schirinzi T, Monfrini E, et al. Association between plasma glucosylsphingosine levels and dyskinesia burden in GBA1-related Parkinson's disease. Neurobiol Dis. 2026 Feb;219:107271.

29. Gleason A, Tayebi N, Lopez G, Sidransky E. No Evidence That Glucosylsphingosine Is a Biomarker for Parkinson's Disease: Statistical Differences Do Not Necessarily Indicate Biological Significance. Mov Disord. 2022 Mar;37(3):653.

30. Sidhu R, Mikulka CR, Fujiwara H, Sands MS, Schaffer JE, Ory DS, et al. A HILIC-MS/MS method for simultaneous quantification of the lysosomal disease markers galactosylsphingosine and glucosylsphingosine in mouse serum. Biomed Chromatogr. 2018 Jul;32(7):e4235.

31. Matsumoto SI, Sato S, Otake K, Kosugi Y. Highly-sensitive simultaneous quantitation of glucosylsphingosine and galactosylsphingosine in human cerebrospinal fluid by liquid chromatography/tandem mass spectrometry. J Pharm Biomed Anal. 2022 Aug 5;217:114852.

32. Dekker N, van Dussen L, Hollak CE, Overkleeft H, Scheij S, Ghauharali K, et al. Elevated plasma glucosylsphingosine in Gaucher disease: relation to phenotype, storage cell markers, and therapeutic response. Blood. 2011 Oct 20;118(16):e118–27.

33. Mirzaian M, Wisse P, Ferraz MJ, Gold H, Donker-Koopman WE, Verhoek M, et al. Mass spectrometric quantification of glucosylsphingosine in plasma and urine of type 1 Gaucher patients using an isotope standard. Blood Cells Mol Dis. 2015 Apr;54(4):307–14.

34. Rolfs A, Giese AK, Grittner U, Mascher D, Elstein D, Zimran A, et al. Glucosylsphingosine is a highly sensitive and specific biomarker for primary diagnostic and follow-up monitoring in Gaucher disease in a non-Jewish, Caucasian cohort of Gaucher disease patients. PLoS One. 2013 Nov 20;8(11):e79732.

35. Irún P, Cebolla JJ, López de Frutos L, De Castro-Orós I, Roca-Espiau M, Giraldo P. LC-MS/MS analysis of plasma glucosylsphingosine as a biomarker for diagnosis and follow-up monitoring in Gaucher disease in the Spanish population. Clin Chem Lab Med. 2020 Apr 28;58(5):798–809.

36. Sato S, Matsumoto SI, Kosugi Y. Quantitation and characterization of glucosylsphingosine in cerebrospinal fluid (CSF), plasma, and brain of monkey model with Gaucher disease. Drug Metab Pharmacokinet. 2023 Dec;53:100530.

37. Tang C, Jia X, Tang F, Liu S, Jiang X, Zhao X, et al. Detection of glucosylsphingosine in dried blood spots for diagnosis of Gaucher disease by LC-MS/MS. Clin Biochem. 2021 Jan;87:79–84.

38. Prinetti A, Loberto N, Chigorno V, Sonnino S. Glycosphingolipid behaviour in complex membranes. Biochim Biophys Acta. 2009 Jan;1788(1):184–93.

39. Russo D, Parashuraman S, D'Angelo G. Glycosphingolipid-Protein Interaction in Signal Transduction. Int J Mol Sci. 2016 Oct 15;17(10):1732.

40. Abdelkarim H, Marshall MS, Scesa G, Smith RA, Rue E, Marshall J, et al. α-Synuclein interacts directly but reversibly with psychosine: implications for α-synucleinopathies. Sci Rep. 2018 Aug 20;8(1):12462.

41. He X, Guan F, Lei L. Structure and function of glycosphingolipids on small extracellular vesicles. Glycoconj J. 2022 Apr;39(2):197–205.

42. Camunas-Alberca SM, Moran-Garrido M, Sáiz J, Gil-de-la-Fuente A, Barbas C, Gradillas A. Integrating the potential of ion mobility spectrometry-mass spectrometry in the separation and structural characterisation of lipid isomers. Front Mol Biosci. 2023 Mar 16;10:1112521.

43. Zheng X, Smith RD, Baker ES. Recent advances in lipid separations and structural elucidation using mass spectrometry combined with ion mobility spectrometry, ion-molecule reactions and fragmentation approaches. Curr Opin Chem Biol. 2018 Feb;42:111–8.

44. Giles K, Ujma J, Wildgoose J, Pringle S, Richardson K, Langridge D, et al. A Cyclic Ion Mobility-Mass Spectrometry System. Anal Chem. 2019 Jul 2;91(13):8564–73.

45. Tu J, Zhou Z, Li T, Zhu ZJ. The emerging role of ion mobility-mass spectrometry in lipidomics to facilitate lipid separation and identification. TrAC Trends in Analytical Chemistry 2019 Jul 1;116:332–9.

46. Dubland JA. Lipid analysis by ion mobility spectrometry combined with mass spectrometry: A brief update with a perspective on applications in the clinical laboratory. J Mass Spectrom Adv Clin Lab. 2021 Dec 13;23:7–13.

47. Pang C, Castro-Gonzales MF, DelHoyo AE, Lee KW. Noncovalent crown ether-assisted separation of stereoisomeric glycosphingosines using cyclic ion mobility spectrometry. Anal Bioanal Chem. 2025 Dec;417(30):6973–82.

48. Zickus MA, Koepke S, Hao C, Chong K, Ryzhov V. The thermochemical studies of protonated amine–crown ether complexes: Extension of the kinetic method. International Journal of Mass Spectrometry. 2012 Feb 15;312:173–8.

49. Bohrer BC, Clemmer DE. Shift reagents for multidimensional ion mobility spectrometry-mass spectrometry analysis of complex peptide mixtures: evaluation of 18-crown-6 ether complexes. Anal Chem. 2011 Jul 1;83(13):5377–85.

50. Li Z, Valentine SJ, Clemmer DE. Complexation of amino compounds by 18C6 improves selectivity by IMS-IMS-MS: application to petroleum characterization. J Am Soc Mass Spectrom. 2011 May;22(5):817–27.

51. Hilderbrand AE, Myung S, Clemmer DE. Exploring crown ethers as shift reagents for ion mobility spectrometry. Anal Chem. 2006 Oct 1;78(19):6792–800.

52. Stow SM, Causon TJ, Zheng X, Kurulugama RT, Mairinger T, May JC, et al. An Interlaboratory Evaluation of Drift Tube Ion Mobility-Mass Spectrometry Collision Cross Section Measurements. Anal Chem. 2017 Sep 5;89(17):9048–55.

53. McCabe JW, Hebert MJ, Shirzadeh M, Mallis CS, Denton JK, Walker TE, et al. THE IMS PARADOX: A PERSPECTIVE ON STRUCTURAL ION MOBILITY-MASS SPECTROMETRY. Mass Spectrom Rev. 2021 May;40(3):280–305.

54. Whyte GF, Vilar R, Woscholski R. Molecular recognition with boronic acids-applications in chemical biology. J Chem Biol. 2013 Jun 1;6(4):161–74.

55. Pham HT, Julian RR. Characterization of glycosphingolipid epimers by radical-directed dissociation mass spectrometry. Analyst. 2016 Feb 21;141(4):1273–8.

56. António JPM , Russo R , Carvalho CP , Cal PMSD , Gois PMP . Boronic acids as building blocks for the construction of therapeutically useful bioconjugates. Chem Soc Rev. 2019 Jul 1;48(13):3513–36.

57. Liu X, Seeberger PH. A Suzuki-Miyaura coupling mediated deprotection as key to the synthesis of a fully lipidated malarial GPI disaccharide. Chem Commun (Camb). 2004 Aug 7;(15):1708–9.

58. Gevorgyan A, Hopmann KH, Bayer A. Lipids as versatile solvents for chemical synthesis. Green Chem. 2021;23(18):7219–27.